International Journal of Science and Research (IJSR)
ISSN (Online): 2319-7064
Index Copernicus Value (2013): 6.14 | Impact Factor (2013): 4.438

Finite Element Analysis of Friction Welding Process for AA7020-T6 and Ti-6Al-4V Alloy: Experimental Validation

A. Chennakesava Reddy

Professor, Department of Mechanical Engineering, JNTUH College of Engineering, Kukatpally, Hyderabad – 500 085, Telangana, India

Abstract: ***The purpose of this work was to assess friction welding of AA7020 and Ti 6Al-4V alloy. Finite element analysis was adopted to analyze the friction welding process. The process parameters were frictional time, frictional pressure, rotational speed and forging pressure. The joints were evaluated for their strength, bulk deformation, penetration and flange formation. The heat affected zone and metal flow across the weld joints were also studied. For friction welding of AA7020-T6 and Ti 6Al-4V alloy, the forging pressure should be less than the frictional pressure or equal.***

Keywords: AA7020-T6, Ti 6Al-4V alloy, frictional time, frictional pressure, rotational speed and forging pressure, friction welding.

1. Introduction

Friction welding has received much attention in the field of manufacturing technology because it allows material combinations to be joined than with any other welding process. In the friction welding process, the developed heat at the interface raises the temperature of workpieces rapidly to values approaching the melting range of the material. Welding occurs under the influence of pressure that is applied when heated zone is in the plastic range [1, 3].

As a rule, all metallic engineering materials which are forgeable can be friction welded. Ti 6Al-4V offers a combination of high strength, light weight, formability and corrosion resistance which have made it a world standard in aerospace applications. In the friction welding of Ti alloys the recrystallization is detected very close to the weldments in the thermal zone. The hardness value increases with this recrystallization zone as the work hardening caused by applied load of forging pressure [4]. It has been reported that that good adhesion characteristics of the welding parts increases the resistance to bulk deformation, thereby involving a large volume of plastically deformed metal [5]. AA7020 is a heat treatable aluminum alloy with zinc added as the main alloying element. This enhances the mechanical property attributes of the material and increases its resistance to fatigue stress. The AA7020 is primarily used in aerospace applications and offers a reasonable machinability. In one of the studies on mechanisms involved in the friction welding of 7056-T6 aluminum alloy [6], severe wear and subsurface circumferential flow have been observed during high-speed sliding under high axial pressures. Further, the intimate contact of nascent surfaces is the principal mechanism of formation of adhesion bonds with consequent wedge formation and mass disruption of the contaminated surfaces.

During the friction welding the material with high temperature may undergo the plastic deformation, large strain and large strain rate under the condition of high axial pressure. The foremost difference between the welding of similar materials and that of dissimilar materials is that the axial movement is unequal in the latter case whilst the similar materials experience equal movement along the common axis. This problem arises not only from the different coefficients of thermal expansion, but also from the distinct hardness values of the dissimilar materials to be joined [7, 8]. The coefficient of thermal expansion of the AA7020 and Ti 6Al-4V alloy, respectively are 23.1 and 9.7 µm/m-^{o}C. The Brinell hardness values of the AA7020 and Ti 6Al-4V alloy are 105 and 334. Heat treatable alloys such as the 7XXX, 2XXX, and 6XXX are vulnerable to critical changes in the Heat Affected Zone (HAZ) due to the heat input during welding. For this reason an extensive study is required to choose appropriate process parameters for friction welding of the AA7020 and Ti 6Al-4V alloy.

This investigation was carried out to study the influence of process parameters on weld strength, bulk deformation and metal flow during the conventional friction welding of the AA7020-T6 and Ti 6Al-4V alloy. Attention was focused on some of the important phenomena that occur during frictional welding under different conditions of rotational speed, frictional pressure, frictional time and forging pressure. The experiments were planned using Taguchi techniques; the frictional welding was modeled using finite element analysis (FEA).

2. Finite Element Modeling

In this study, ANSYS WORKBENCH (15.0) software was used in the coupled deformation and heat flow analysis during friction welding of the AA7020-T6 and Ti 6Al-4V alloy. An axisymmetric 3D model of the AA7020-T6 and Ti 6Al-4V alloy s of 25.4 mm diameter and 100 mm length were made using ANSYS workbench as shown in figure 1. Tetrahedron elements were used to mesh the AA7020-T6 and Ti 6Al-4V alloy rods [9]. The rotating part (AA7020-T6) and the non-rotating part (Ti 6Al-4V alloy) were meshed with 3298 elements / 14904 nodes and 3672 elements / 16493 nodes correspondingly.

The boundary conditions are mentioned in figure 2. First the transient thermal analysis was carried out keeping the Ti 6Al-4V alloy rod stationary and the AA7020-T6 rod in rota-

tion. The coefficient of friction 0.2 was applied at the interface of the AA7020-T6 and Ti 6Al-4V alloy rods. The convection heat transfer coefficient was applied on the surface of two rods. The heat flux calculations were imported from ANSYS APDL commands and applied at the interface. The temperature distribution was evaluated. The thermal analysis was coupled to the static structural analysis. For the structural analysis the rotating (AA7020-T6) rod was brought to stationary and the forging pressure was applied on the Ti 6Al-4V alloy rod along the longitudinal axis. The Ti 6Al-4V alloy rod was allowed to move in the axial direction. The structural analysis was carried out for the principle stresses and strains, equivalent stress and equivalent strain, and bulk deformation. The contact analysis was also carried out to estimate the depth of penetration and sliding of the material at the interface.

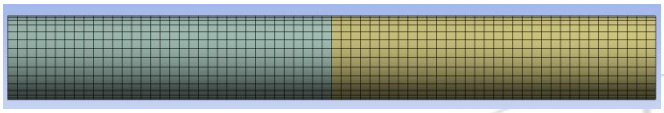

Figure 1: Finite element modeling of friction welding

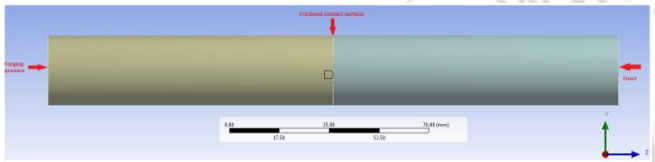

Figure 2: The boundary conditions

The modeling and analysis of the friction welding was carried out as per the design of experiments using Taguchi techniques. The process parameters and their levels are given table-1. The orthogonal array (OA), L9 was selected for the present work. The parameters were assigned to the various columns of O.A. The assignment of parameters along with the OA matrix is given in Table 2.

Table 1: Process parameters and levels

Factor	Symbol	Level–1	Level–2	Level–3
Frictional Pressure, MPa	A	25	30	35
Frictional time, Sec	B	2	3	4
Rotational speed	C	1200	1500	1800
Forging pressure, MPa	D	31.25	37.5	43.75

Table 2: Orthogonal Array (L9) and control parameters.

Trial No.	A	B	C	D
1	1	1	1	1
2	1	2	2	2
3	1	3	3	3
4	2	1	2	3
5	2	2	3	1
6	2	3	1	2
7	3	1	3	2
8	3	2	1	3
9	3	3	2	1

3. Results and Discussion

The experiments were repeated twice with two meshing conditions to keep errors least in the finite element analysis. The results obtained from the finite element analysis were verified experimentally on the selective trial. The statistical Fisher's test was carried out to find the acceptable all process parameters at 90% confidence level.

3.1 Influence of parameters on temperature distribution

Table – 3 gives the ANOVA (analysis of variation) summary of temperature distribution. The friction time by itself would contribute 81.28% of the total variation in the temperature raised due to friction. The frictional pressure gave 17.25% of the total variation in the temperature. Even though the rotational speed and forging were satisfactory statistically, but their influences were negligible.

Table 3: ANOVA summary of the temperature distribution

Source	Sum 1	Sum 2	Sum 3	*SS*	*v*	*V*	*F*	*P*
A	4404.17	5252.55	6088.16	236323	2	118161.5	15023.33	17.25
B	3452.49	5185.72	7106.67	1113731	2	556865.7	70801.22	81.28
C	5343.73	5350.87	5050.28	9806.56	2	4903.28	623.41	0.71
D	5450.68	4429915	15744.88	10263.78	2	5131.89	652.48	0.75
e				70.78	9	7.8652	1.00	0.01
T	18651.07	4445704	33989.99	1370196	17			100

Note: SS is the sum of square, v is the degrees of freedom, V is the variance, F is the Fisher's ratio, P is the percentage of contribution and T is the sum squares due to total variation.

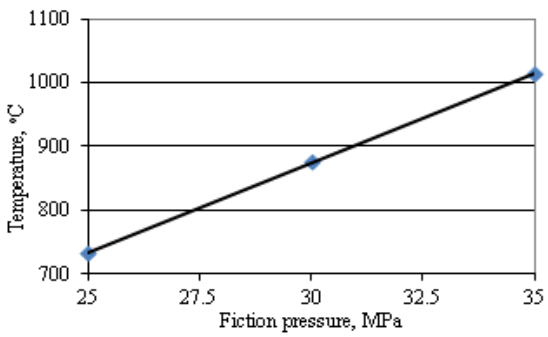

Figure 3: Influence of frictional pressure on temperature.

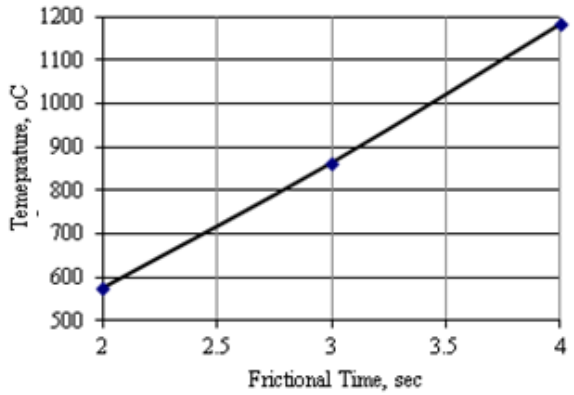

Figure 4: Influence of frictional time on temperature

The temperature developed in the welding rods was directly proportional to the frictional pressure and frictional time as shown in figure 3 & 4. In fact this is a natural phenomenon. The conditions of trial 9 gave the highest temperature (1380°C) generation and trial 1 gave the lowest temperature (484°C) generation in the rods. For trial 9, the frictional pressure and time were, respectively 35 MPa and 4 sec; whereas these were 25 MPa and 2 sec respectively for the trial 1 (figure 5).

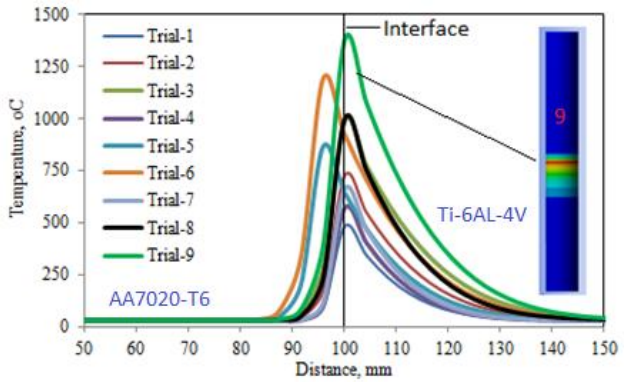

Figure 5: Temperature distribution during different trials.

3.2 Influence of parameters on equivalent stress

The ANOVA summary of the equivalent stress is given in Table 4. However, the major contribution (78.54%) was of friction time towards variation in the effective stress. The second parameter was frictional pressure (19.97% of variation). The influence of other factors was negligible.

Table 4: ANOVA summary of the equivalent stress

Source	Sum 1	Sum 2	Sum 3	*SS*	*v*	*V*	*F*	*P*
A	5969.51	7164.51	8375.53	482418.15	2	241209.07	10396.77	19.97
B	4820.53	7099.02	9590	1896907.9	2	948453.95	40880.95	78.54
C	7280.89	7318.33	6910.33	16954.46	2	8477.23	365.39	0.7
D	7443.59	8242558.8	21509.55	18733.49	2	9366.745	403.73	0.77
e				208.8035	9	23.200389	1.00	0.02
T	25514.52	8264140.7	46385.41	2415222.8	17			100

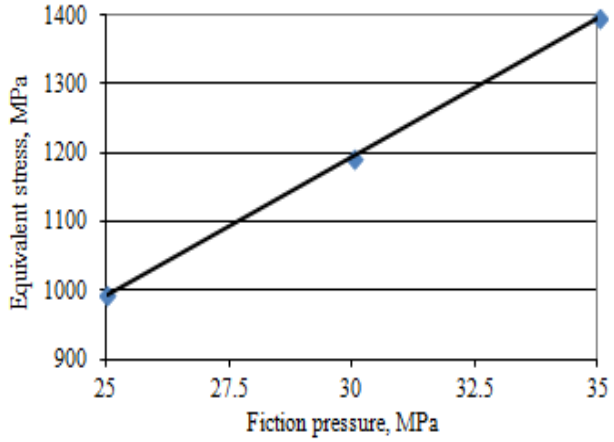

Figure 6: Influence of frictional pressure on equivalent stress.

The equivalent stress induced in the welding rods was directly proportional to the frictional pressure and frictional time as shown in figure 6 & 7. It can be observed from figure 8 that the stress induced in the heat affected zone (HAZ) was higher in all the welds than that in the parent metal. This was due to recrystallization in the HAZ. The stresses induced in the HAZ were of thermal stresses due to frictional heat and of structural stresses owing to applied forging pressure. The residual stresses must be relieved by the heat treatment otherwise the joints may fail.

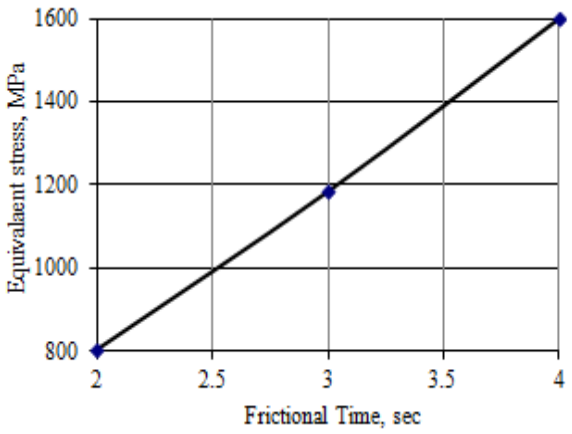

Figure 7: Influence of frictional time on equivalent stress.

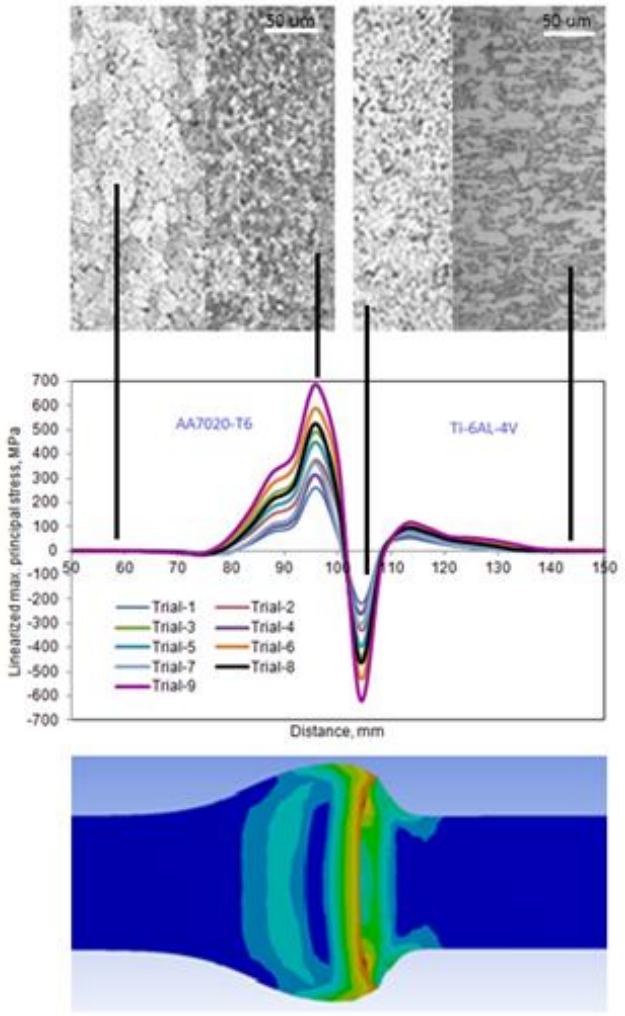

Figure 8: Linearized maximum principle stress induced in weld rods

The conditions of trial 9 had induced the highest effective stress (1868.30 MPa) and trial 1 had induced the lowest effective stress (669.99 MPa) in the rods as shown in figure 9. During friction heating stage any surface irregularities are removed, the temperature increases in the vicinity of the welded surfaces, and an interface of visco-plastic aluminum is formed. During forging pressure stage there is significant thermo-plastic deformation of aluminum in the contact area. In result of this is formation of a flange-like flash. The process of welding takes place due to the plastic and diffusion effects.

	FEA results
1	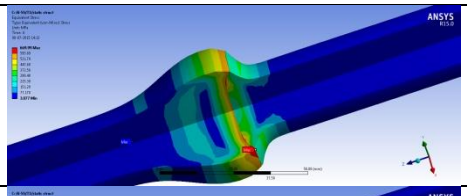
2	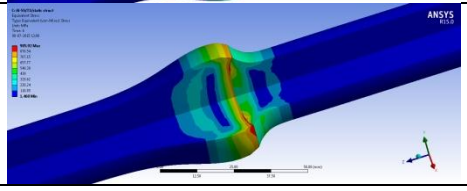

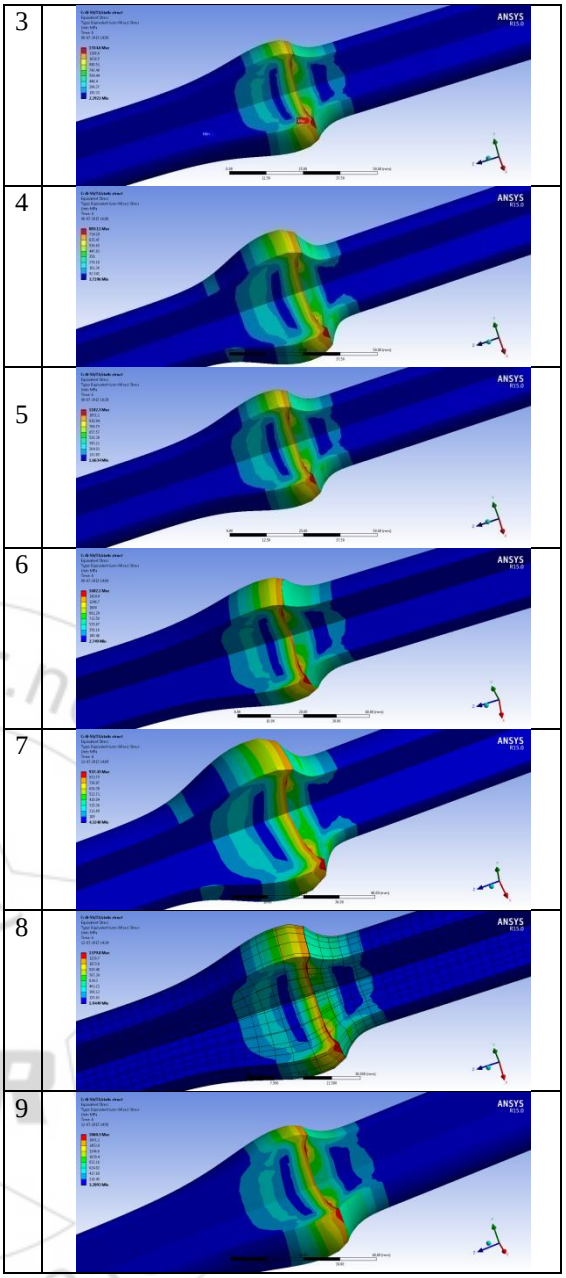

Figure 9: Equivalent stress values under different trials

Table 5: ANOVA summary of the bulk deformation

Source	Sum 1	Sum 2	Sum 3	*SS*	*v*	*V*	*F*	*P*
A	1.37	1.618	1.89	0.03	2	0.015	12.40	11.21
B	0.79	1.554	2.54	0.26	2	0.13	107.50	90.77
C	1.66	1.688	1.53	0	2	0	0	0.84
D	1.72	0.43	4.88	0.01	2	0.005	4.13	4.3
e				0.01	9	0.0012	1.00	-7.12
T	5.54	5.29	10.85	0.29	17			100

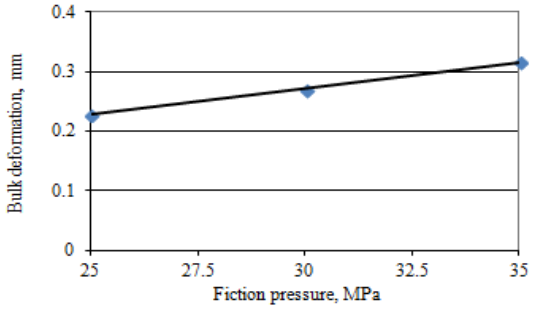

Figure 10: Influence of frictional pressure on deformation.

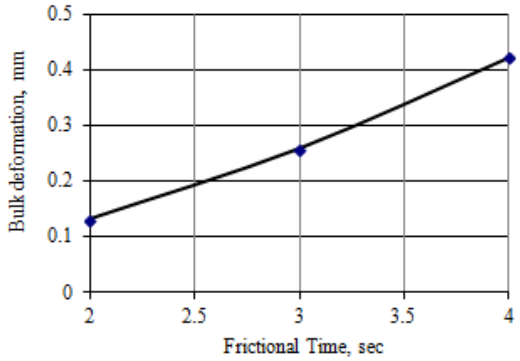

Figure 11: Influence of frictional time on deformation.

3.3 Influence of parameters on bulk deformation

The ANOVA summary of the directional deformation is given in Table 6. The major contribution (90.77%) was of frictional time towards variation in the bulk deformation. the second contribution (11.21%) was of frictional pressure towards variation in the bulk deformation The influence of rotational speed and forging pressure were negligible. The bulk deformation was with an increase in the frictional pressure and frictional time as shown in figure 10 & 11. In the first numerical iteration the external load would generate uniform pressure on the contact surface and consequently linearly changing heat flux. For the next iteration the pressure distribution on contact surface was calculated Using ANSYS workbench. It was observed that the deformation concentrates mainly near the frictional surface. The extruded shape gradually was formed near the welded joint during the welding process. The extruded shape was asymmetric, as shown in figure 12. The tendency of flange formation was higher with AA7020 than with Ti 6Al-4V alloy. This was due to difference in the thermal conductivity and thermal expansion of the two materials. The bulk deformation was found to be maximum (0.496 mm) with conditions of trial 9; whereas it was 0.109 mm with the trial 1 as shown in figure 12.

	FEA results
1	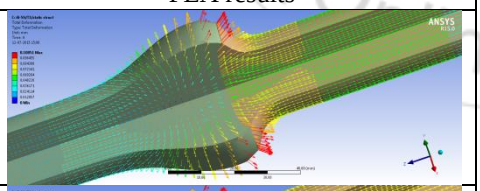
2	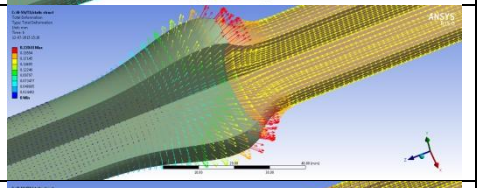
3	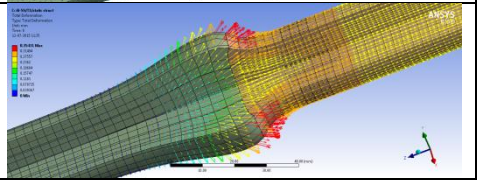

4	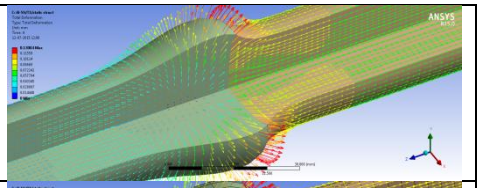
5	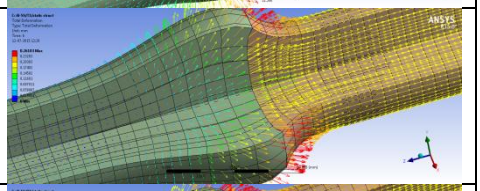
6	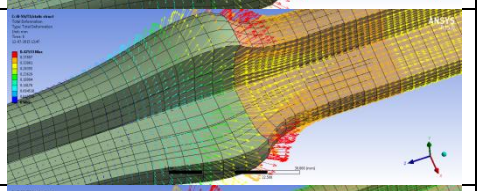
7	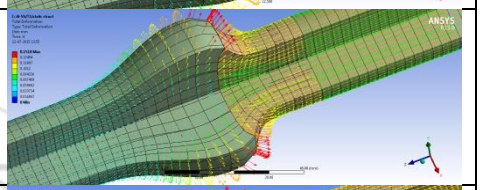
8	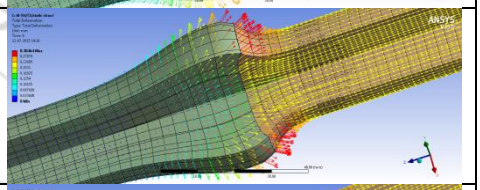
9	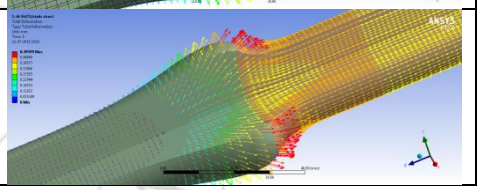

Figure 12: Bulk deformation values under different trials

3.4 Influence of parameters on penetration and sliding

In friction welding of AA7020-T6 and Ti 6Al-4V alloy, only Aa7020-T6 was consumed in the form of flash due to softer material and also due to higher thermal conductivity and coefficient of thermal expansion, as most of the heat generated at the interface was transferred to AA7020-T6. Deformation of Ti 6Al-4V alloy was negligible due to its higher hardness value, and higher melting point as shown in figure 16. In the case of trail 1 the interface layer has not produced a good metallic bond between AA7020-T6 and Ti 6Al-4V alloy due to lack of penetration. In the case of trail 9 the interface layer has produced a good metallic bond between AA7020-T6 and Ti 6Al-4V alloy on account of deep penetration (figure 13). In trail 6 also a good penetration was observed. A closer look at the penetration and sliding images shows that the failure of good bonding has taken place largely by interface separation. Some problems, such as inconsistency of the weld results, were encountered with this combination of materials. One factor may be the randomly varying relative motions between welding parts, which could result in an uneven rate of heat generation. Due to this uneven rate of heat input, the amount of melt-off for each cycle for welding this combination of AA7020-T6 and Ti 6Al-4V alloy.

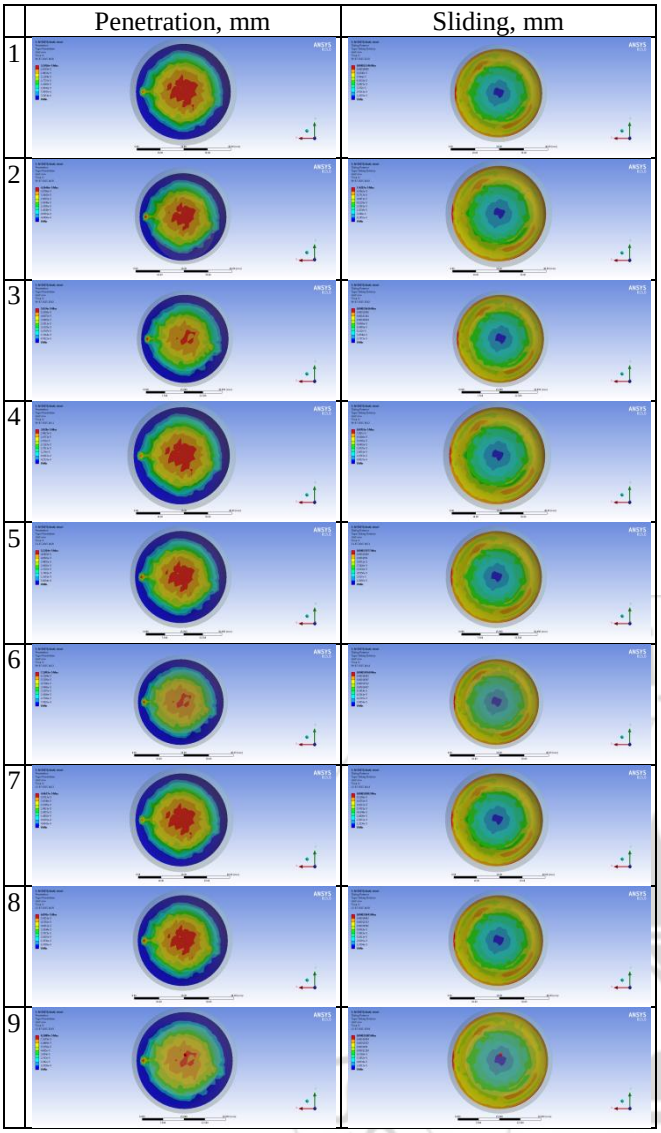

Figure 13: Penetration and sliding values under different trials.

A typical example of friction welded AA70720-T6 and Ti 6Al-4V alloy is shown in figure 14. The aircraft rivets were made of Ti 6Al-4V alloy and AA7020-T6. The friction welding was carried out using the experimental conditions of trial 9.

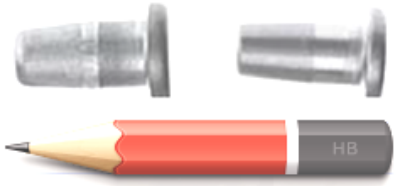

Figure 14: Friction welded aircraft rivets

4. Conclusions

This study shows that the AA7020-T6 and Ti 6Al-4V alloy is good if the operating conditions: frictional pressure of 35 MPa, frictional time of 4 sec, rotational speed of 1500 rpm and forging pressure of 31.25 MPa. For friction welding of AA7020-T6 and Ti 6Al-4V alloy, the forging pressure should be less than the frictional pressure or equal. For this condition of welding there was good penetration and sliding of materials at the welding interface resulting a good mechanical bonding. It is also recommended that the welded parts must be stress relieved using appropriate heat treatment process.

5. Acknowledgements

The author acknowledges with thanks University Grants Commission (UGC) – New Delhi for sectioning R&D project.

References

[1] V. Srija and A. C. Reddy, "Finite Element Analysis of Friction Welding Process for 2024Al Alloy and UNS C23000 Brass," International Journal of Science and Research, vol.4, no.5, pp.1685-1690, 2015.
[2] T. Santhosh Kumar and A. C. Reddy, "Finite Element Analysis of Friction Welding Process for 2024Al Alloy and AISI 1021 Steel," International Journal of Science and Research, vol.4, no.5, pp.1679-1684, 2015.
[3] A. Raviteja and A. C. Reddy, Finite Element Analysis of Friction Welding Process for UNS C23000 Brass and AISI 1021 Steel, International Journal of Science and Research, vol.4, no.5, pp.1691-1696, 2015.
[4] C. Kwietniewski, J. F. dos Santo, A.A. M da Silva, L. Pereira, T. R. Strohaecker and A. Reguly " Effect of Plastic Deformation on the Toughness Behaviuor of Radial Friction Welds of Ti-6Al-4V-0.1Ru Titanium Alloy," Materials Science & Engineering A,vol.417, pp 49-55, 2006.
[5] I.V. Kraghelsjii, "Friction and wear," Translated from Russian Publishers, Butterworth, Inc., Washington. D.C, 1965.
[6] W. Li and F. Wang, "Modeling of continuous drive friction welding of mild steel", Materials Science and Engineering A, vol.528, pp.5921-5926, 2011.
[7] A. Chennakesava Reddy, "Fatigue Life Prediction of Different Joint Designs for Friction Welding of 1050 Mild Steel and 1050 Aluminum," International Journal of Scientific & Engineering Research, vol.6, no.4, pp.408-412, 2015.
[8] A. Chennakesava Reddy, Fatigue Life Evaluation of Joint Designs for Friction Welding of Mild Steel and Austenite Stainless Steel, International Journal of Science and Research, vol.4, no.2, pp.1714-1719, 2015.
[9] Chennakesava R Alavala, Finite Element Methods: Basic Concepts and Applications, PHI Learning Solutions Private Limited, New Delhi, 2008.